Journal of Food and Drug Analysis

Volume 28 | Issue 4 Article 4

2020

Functionalized gold nanoparticles for sensing of pesticides: A review

Functionalized gold nanoparticles for sensing of pesticides: A review

Cover Page Footnote

This work was financially supported by the Ministry of Science and Technology of Taiwan under contract number MOST 108-2113-M-017-003 and 109-2113-M-143-002.

REVIEW ARTICLE

Functionalized gold nanoparticles for sensing of pesticides: A review

Wei-Bin Tseng [a], Ming-Mu Hsieh [b], Che-Hsie Chen [c], Tai-Chia Chiu [c,*], Wei-Lung Tseng [d,e,**]

[a] Department of College of Ecology and Resource Engineering, Wuyi University, Fujian, China
[b] Department of Chemistry, National Kaohsiung Normal University, Taiwan
[c] Department of Applied Science, National Taitung University, Taitung, Taiwan
[d] Department of Chemistry, National Sun Yat-sen University, No. 70, Lien-hai Road, Gushan District, Kaohsiung, 80424, Taiwan
[e] School of Pharmacy, Kaohsiung Medical University, No. 100, Shiquan 1st Road, Sanmin District, Kaohsiung, 80708, Taiwan

Abstract

Pesticides are a family of non-biodegradable chemical compounds which widely used in agriculture to control pests and increase yield production. However, overuse or abuse of pesticides and their metabolites may cause potential toxicity for the environment as well as human health and all other living organisms, even at deficient concentrations. Consequently, the development of sensors for monitoring these compounds is significant. Recently, nanoparticles-based sensors have been extensively employed as a potential alternative or complementary analytical tool to conventional detection methods for pesticides. Among them, gold nanoparticles (AuNPs) owing to their unique optical properties have been developed as smart sensors with high selectivity, sensitivity, simplicity, and portability. These comprehensive reviews have summarized various studies performed based on different detection strategies, i.e., colorimetric, fluorescence, surface-enhanced Raman scattering, and electrochemical, using AuNPs as sensing probes for pesticide analysis in various matrices. Additionally, the current challenges and future trends for developing novel AuNPs-based sensors for the detection of pesticides are also discussed.

Keywords: Colorimetry, Electrochemical, Fluorescence, Gold nanoparticles, Pesticides, Surface-enhanced Raman scattering

1. Introduction

Pesticides are a large and heterogeneous group of heavily employed chemicals in modern agriculture for protecting crops, controlling insect pests, and improving productivity [1]. In terms of their chemical structures, pesticides can be classified into four leading groups, including organochlorines, organophosphorus, carbamate, chlorophenols, and synthetic pyrethroids [2]. If concerned with pesticides' function, they can be categorized into five types that include insecticides, herbicides, fungicides, rodenticide, and nematocides [3–5]. Many toxic pesticides have been extensively used in agriculture due to their low cost and high effectiveness [1,2]. However, the overuse, abuse, and misuse of pesticides lead to their residues and metabolites' release, causing the adverse effect on the ecological system and human health [6]. Even exposure to very low pesticide levels could be highly involved in food and water safety [7]. Additionally, some of the pesticides, identified as endocrine disruption, have been implicated with neurotoxicity, genotoxicity, mutagenicity, and carcinogens [8–10]. Based on the consideration of toxic pesticides' threats to human health and the environment, it is urgent to develop sensitive, selective, low-cost, and affordable analytical methods to monitor their level in real-world samples.

Received 9 May 2020; revised 23 July 2020; accepted 6 August 2020.
Available online 1 December 2020

* Corresponding author at: Department of Applied Science, National Taitung University, 369, Section 2, University Road, Taitung, 95092, Taiwan. Tel: +886 89 517990; Fax: +886 89 518108.

** Corresponding author at: Department of Chemistry, National Sun Yat-sen University, No. 70, Lien-hai Road, Gushan District, Kaohsiung, 80424, Taiwan. Fax: +011 886 7 5254644.
E-mail addresses: tcchiu@nttu.edu.tw (T.-C. Chiu), tsengwl@mail.nsysu.edu.tw (W.-L. Tseng).

https://doi.org/10.38212/2224-6614.1092

Current analytical methods used to determine pesticides and their metabolites mainly include three parts of quick, easy, cheap, effective, rugged and safe (QuEChERS) extraction, separation techniques (gas chromatography and high-performance liquid chromatography), and mass spectrometry (e.g., quadrupole ion trap and time-of-flight instruments) [11,12]. Although offering satisfactory sensitivity and excellent separation efficiency, most mass spectrometry-related approaches still suffer from time-consuming sample preparation, sophisticated instrumentation, and required skilled operators [13]. More importantly, these methods are hard to transform into a portable device for on-site detection. Recently, ligand-capped gold nanoparticles (AuNPs) with a size range from 1 to 100 nm have attracted tremendous interests since they provide high molar extinction coefficients ($>10^8$ M^{-1} cm^{-1}), size-dependent optical properties, strong Rayleigh scattering, and easy functionalization. These features enable ligand-capped AuNPs to be well-suited for the practical applications in photonics [14–16], electronics [17,18], biosensing [18–20], bioimaging [21,22], and nanomedicine [23–26]. In addition to these applications mentioned above, ligand-capped AuNPs also serve as a sensing platform for colorimetric, fluorometric, and electrochemical detection of a broad range of analytes from metal ions and small biomolecules to protein and DNA macromolecules. The sensing mechanism of ligand-capped AuNPs can be divided into three strategies: (1) a target analyte induces the aggregation of ligand-capped AuNPs *via* the coordination interaction between two ligands and a target analyte; (2) a target analyte triggers the removal of a colloidal stabilizer from the nanoparticle surface *via* the formation of Au–S bonds, resulting in the salt-mediated assembly of ligand-capped gold nanoparticles; (3) a target analyte drives the liberation of a recognition molecule from the nanoparticle's surface through the complexation reaction. The aggregation of ligand-capped AuNPs can promote a redshift in surface Plasmon resonance, a restoration in fluorescence peak, and an enhancement in Raman scattering. Taking these advantages, researchers have developed different kinds of ligand-capped AuNPs for probing pesticides in real-world samples. In this review, we present a comprehensive discussion associated with the recent advancements in the use of unmodified and functionalized AuNPs to detect pesticides. To the author's knowledge, there is no systematic review covering such topics. We especially emphasize integrating the colorimetric, fluorescence, surface-enhanced Raman scattering (SERS), and electrochemical strategies (Fig. 1) with ligand-capped AuNPs for the determination of pesticides.

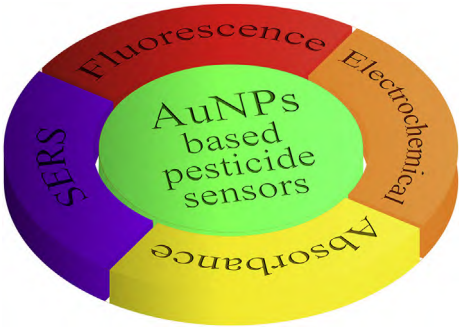

Fig. 1. Schematic illustration for various AuNPs-based sensing strategies for the pesticide detection.

2. Synthesis of AuNPs and their modification

Gold has different oxidation states that include Au^{+3} (auric), Au^{+1} (aurous), and atomic Au^0. Since AuNPs consist of numerous Au^0, the synthetic procedure involves the reduction of Au^{+3} or Au^{+1} to Au^0 with a reducing agent. Examples of reducing agents include citric acid [18,27,28], ascorbic acid [29,30], sodium borohydride [31], oxalic acids [32,33], sulfites [34,35], and hydrogen peroxide [27,36]. At the beginning of the process synthesis, chloroauric acid ($HAuCl_4$) is frequently employed as a precursor chemical in the preparation of the AuNPs, and it can be purchased from chemical companies or obtained from the reaction of aqua regia and gold foil. Also, capping ligands are needed in a precursor solution to prevent the formed AuNPs from aggregation and further growth during the synthetic process. The capping ligands enable the AuNPs to have sufficient electrostatic repulsion, steric hindrance, or both to be dispersed in an aqueous solution [37–39]. Thiol-terminated small molecules [37,40], trisodium citrate [41,42], surfactants [43,44], polymers [38,45], phosphate-containing nucleotides [46,47], and phosphorus ligands [48] are exemplified by capping ligands. It is interesting to emphasize that several capping ligands serve as a reducing agent and a stabilizing agent [49]. After mixing $HAuCl_4$ with a weak reducing agent in the presence of capping ligands, the resultant solution is commonly treated with heating [50], microwave irradiation [51], and UV light exposure [52]. Once substituting a weak reducing agent with a strong one, the reaction simply proceeds at ambient temperature [53,54]. UV–visible and X-ray spectroscopies have been implemented for monitoring the nucleation and growth of the AuNPs [55]. Electron microscopic and optical spectroscopic techniques can provide detailed information associated with the

morphology, compositions, valence state, and optical properties of the AuNPs [56,57]. Moreover, single-particle inductively coupled plasma mass spectrometry (ICP-MS) has been adopted for accurate quantification of the molar and particle number concentrations of the AuNPs [58,59]. The measurement of zeta potential of the AuNPs can help the investigators to assess whether they are present in the dispersed state [60]. The purification of the AuNPs can be performed by filtration, centrifugation, dialysis, and separation techniques [61]. A more detailed characterization of the AuNPs has been reviewed in the recent literature [62].

Faraday has pioneered the development of the methodology for producing 5 nm-sized AuNPs from the reduction of $HAuCl_4$ in the presence of the phosphorus-ether solution [63]. During the synthetic process, the mixed solution's color varied from brown, grey, purple, to deep red, which can be easily visualized by the naked eye. This breakthrough opens the door to the synthesis of stable AuNPs and motivates the researchers to design new synthetic routes. The Turkevich method is one of the most common ones used for the reproducible and simple synthesis of approximately 10–50 nm AuNPs with a spherical shape [27]. The formed citrate-capped AuNPs and their surface modification are intensively implemented as a colorimetric reporter to sense organophosphate pesticides. It is worth emphasizing that the preparation of citrate-capped gold nanoparticles is straightforward and simple without high-cost dedicated equipment and a great experience. Besides, the cost for 60 mL of 2.57 nM citrate-capped gold nanoparticles is only *ca.* US$ 0.61. In comparison to the Turkevich method, the AuNPs produced from the seed-mediated growth method [64], Brust-Schiffrin approach [31], electrochemical techniques [65–67], ionic liquid-related preparation [68–70], and biological molecule-mediated synthesis [71–73] are rarely utilized as a platform for the detection of organophosphate pesticides. Fig. 2 reveals the above-mentioned synthetic methods. Accordingly, in the review article, we focus on the detailed discussion of the Turkevich method. Briefly, the Turkevich method involves injecting trisodium citrate into a boiling solution of $HAuCl_4$ under reflux and vigorous stirring. Immediately, rapid nucleation occurs in the initial stage, followed by the aggregation of the nuclei. Next, the formed bigger particles undergo slow diffusion growth by reducing gold ion precursor and further coalescence. Finally, the resultant particles undergo rapid growth to form a fixed size of the AuNPs. The as-prepared citrate-capped AuNPs exhibit the surface plasmon band (SPR) in the visible regions. The mechanism of gold nanoparticle formation mentioned above has been demonstrated using small-angle X-ray scattering (SAXS) and X-ray absorption near-edge spectroscopy (XANES) employing synchrotron radiation [74]. The particle size and size distribution of the AuNPs were reported to be heavily connected with the ratio of $HAuCl_4$ to sodium citrate [75,76], solution pH [77], and synthetic temperature [78]. Although the Turkevich method provides highly reproducible and straightforward for spherical particles' production, the resultant citrate-capped AuNPs are easy to aggregate in a high-ionic-strength solution. Thus, it is required to modify the surface of citrate-capped AuNPs through the ligand-change reaction or stabilizers' adsorption. Examples of colloidal stabilizers include DNA aptamer [79,80], proteins [81,82], neutral surfactants [83,84], adenosine triphosphate [85], cysteine [86], lipoic acid [87], p-nitroaniline dithiocarbamate [88]. Among the stabilizers and capping ligands mentioned above, the DNA aptamers-, adenosine triphosphate-, cysteine-, lipoic acid- and p-nitroaniline dithiocarbamate-modified AuNPs have been utilized for colorimetric assay of organophosphate pesticides that will be discussed in the following section. In addition to using citrate as a reducing and stabilizing agent, D'Souza et al. reported the preparation of ascorbic acid-capped AuNPs through the hydrothermal reduction of $HAuCl_4$ with ascorbic acid at 100 °C for 10 min [89]. The SPR band of the ascorbic acid-capped AuNPs was centered at 525 nm with a particle size of 14.5 nm. Park et al. incubated heparin with $HAuCl_4$ at 60 °C for 20 h, resulting in 20 nm-sized AuNPs with the SPR band of 524 nm [90]. Likewise, heparin behaved as a reducing and stabilized ligand for the synthesis of the AuNPs. Barman et al. synthesized highly stable AuNPs through trichloroacetic acid-triggered reduction of $HAuCl_4$ in the presence of cetyltrimethylammonium bromide (CTAB) [91]. The formed CTAB-capped AuNPs kept dispersed for more than six months. The ascorbic acid-, heparin- and CTAB-capped AuNPs mentioned above have been demonstrated to be powerful for sensing organophosphate pesticides. The sensing procedure will be discussed in the next section.

3. Detection strategies for pesticides based on gold nanoparticles

3.1. Colorimetric assays

The AuNP-related colorimetric assay is a powerful method for the naked-eye detection of numerous analytes due to their large molar extinction

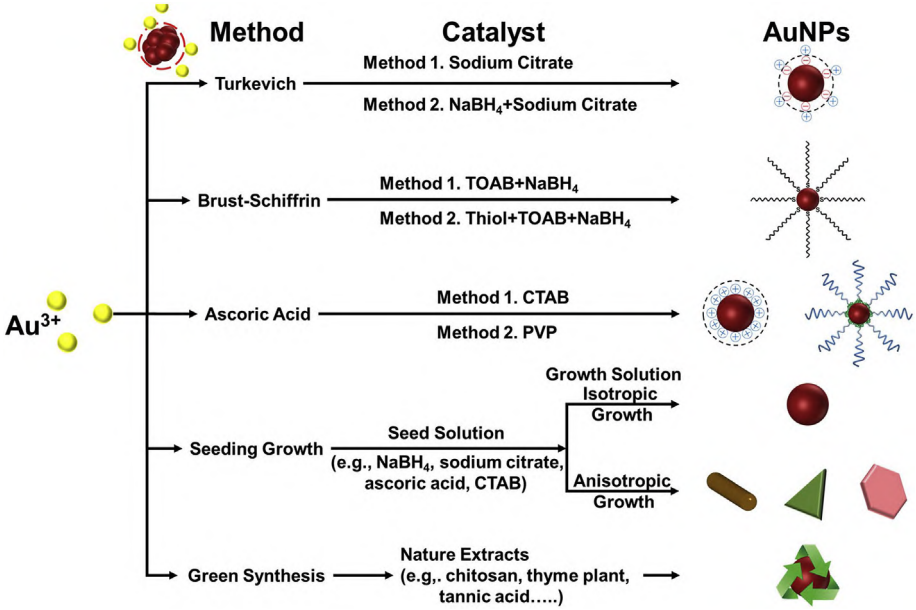

Fig. 2. Summary of the classical methods for the synthesis of AuNPs with different size, shape, and capping ligands.

coefficient [92]. The localized surface Plasmon resonance wavelength of AuNPs is highly susceptible to their aggregation degree and particle size. The presence of the target analyte induces the change in color and surface plasmon resonance wavelength of AuNPs as a consequence of either the conversion from dispersed to aggregated nanoparticles or the disassembly of aggregated nanoparticles, as shown in Fig. 3 [93]. Based on this sensing mechanism, AuNP-based colorimetric sensors have been well-developed for pesticide detection and showed their advantages of rapidity, simplicity, convenience, cost-effectiveness, and visualization by naked-eyes summarized in Table 1. Xu et al. [94] found that acetamiprid molecules were capable of directly attached on the surface of citrate-capped AuNPs, leading to the nanoparticle aggregation and color change. The visualized color change of citrate-capped AuNPs from red to blue was well-suited for determining the concentration of acetamiprid in an aqueous solution. This method was successfully applied to detect acetamiprid in vegetables. Aptamers are short single-stranded oligonucleotides (RNA or DNA) with a specific binding affinity towards their target analytes, and they developed through systematic evolution of ligands by exponential enrichment method [95–97]. Weerathunge et al. [98] demonstrated an aptamer-nanozyme for fast, highly selective, and sensitive detection of acetamiprid based on the inhibition of the peroxidase-like activity of AuNPs. Pesticides-specific aptamer modified on AuNPs also has been developed as apatsensors for colorimetric detection of phorate [99], omethoate [80], malathion [100] and acetamiprid [101] with high selectivity and sensitivity. Dong et al. [102] developed a dual strategy for the fluorescent and visual detection of cyanazine based on the quantum dots (QDs)-AuNPs sensing system. In the presence of cyanazine can induce the aggregation of AuNPs with a color change from red to blue. Fahimi-Kashani et al. [103] demonstrated a colorimetric sensor array for monitoring five organophosphate pesticides based on aggregation behaviors of citrate-AuNPs at different pH values and ionic strengths, as shown in Fig. 4. Rana et al. [104] explored ligand exchange reactions on citrate-AuNPs with a similar concept for colorimetric detection of acephate, phenthoate, profenofos, acetamiprid, chloronitrile, and cartap in water and vegetable samples. Baek et al. [105] designed a portable system for the detection of tebuconazole based on the aggregation of citrate-AuNPs. The colorimetric sensors based on the aggregation of citrate-AuNPs was also used for the detection of carbendazim [106] and chlorothalonil [107]. Wu et al. [108] showed a colorimetric method for parathion analysis based on the enzymatic hydrolysis reaction of acetylcholinesterase (AChE) and the dissolution of AuNPs in Au^{3+}-cetyltrimethylammonium bromide solutions. The activity of AChE is inhibited in the presence of parathion to induce the decreases in both the concentration and size of the AuNPs with noticeable color changes from red to light pink or red to colorless. By loading AuNPs on a cellulose paper, a dipstick could be used for the colorimetric detection of parathion by

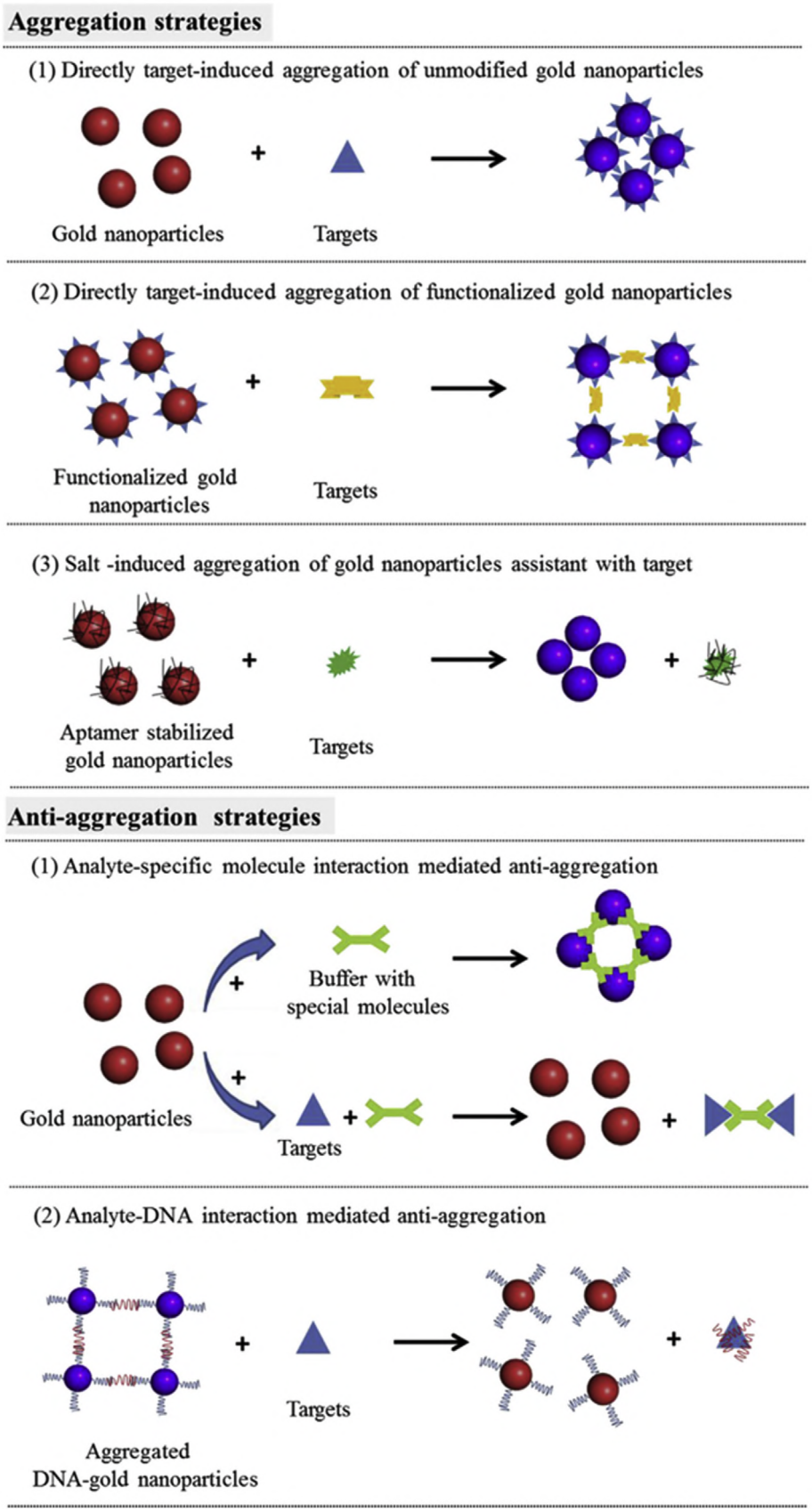

Fig. 3. Typical strategies of colorimetric detection mechanism with gold nanoparticles. Reproduced with permission from Ref. [93].

Table 1. AuNPs based colorimetric sensors for pesticides detection.

Pesticides	Probes	Linear ranges	LODs	Matrix	Ref.
Acetamiprid	Citrate-AuNPs	0.66–6.6 μM 6.6–66 μM	0.044 μM	Green vegetables, Eggplant, Cucumber	[94]
Acetamiprid	Apt-AuNPs	0.1–10 μg/mL	1.8 μg/mL	–	[98]
Phorate	Apt-AuNPs	0.01 nM–1.3 μM	0.01 nM.	Apple	[99]
Omethoate	Apt-AuNPs	0.1–10 μM	0.1 μM	Soil	[80]
Malathion	Apt-AuNPs	0.01–0.75 nM	1.94 pM	Tap water, Lake water, Apple	[100]
Acetamiprid	Apt-AuNPs	10–160 μg/mL	1.02 μg/mL	Tomato, Wastewater	[101]
Cyanazine	QDs-AuNPs	2.0–9.0 μM	0.2201 μM	Tap water, River water, Cabbage	[102]
Azinphos-methyl	Citrate-AuNPs	80 – 400 ng/mL	75 ng/mL	Rice, Paddy water	[103]
Chlorpyrifos		12 – 80 ng/mL	118 ng/mL		
Fenamiphos		80–400 ng/mL	75 ng/mL		
Pirimiphos-methyl		40–800 ng/mL	30 ng/mL		
Phosalone		40–320 ng/mL	37 ng/mL		
Acephate	Citrate-AuNPs	10–900 μM	0.346 μM	Tap water,	[104]
Phenthoate		0.01–1.50 μM	3.0 nM	Canal water,	
Profenofos		1.0–200 μM	0.6 μM	River water,	
Acetamiprid		0.001–0.15 μM	0.624 nM	Cabbage,	
Chloronitrile		1.0–1000 μM	0.375 μM	Tomato,	
Cartap		0.05–1.50 μM	17 nM	Potato	
Tebuconazole	Citrate-AuNPs	0–1.0 μg/mL	52.0 ng/mL	–	[105]
Carbendazim	Citrate-AuNPs	10–600 ng/mL	3.4 ng/mL	Cabbage, Apple	[106]
Chlorothalonil	Citrate-AuNPs	5–100 ng/mL	3.6 ng/mL	Cucumber	[107]
Parathion	AChE-AuNPs-Au^{3+}-CTAB	15–65 ng/mL, 140–1000 ng/mL	0.7 ng/mL (2.4 nM)	Apple washing solution, Tap water, Sea water	[108]
Zineb	AuNPs	0.0008–0.020 μg/mL	0.00055 μg/mL	River water, Tap water, Well water, soil	[109]
Ziram	AuNPs	0.12–2.52 ng/mL	0.06 ng/mL	Well water, River water, Soil, Potato, Carrot, Wheat, Paddy soil	[110]
Pymetrozine	Melamine-AuNPs	10–1000 nM	10 nM	Tap water, Lake water, Green tea, Apple juice	[111]
Deltamethrin	2-mercapto-6-nitrobenzothiazole -AuNPs	0.005 – 1 μM	0.005 μM	Cherry, Mini tomato	[112]
Glyphosate	Cysteamine-AuNPs	0.001–1000 μg/mL	0.026 μg/mL	Spinach leaf, Corn leaf, Apple peel	[113]
Pencycuron	6-aza-2-thiothymine-AuNPs	2.5–100 μM	0.42 μM	Water, Rice, Potato, Cabbage	[114]

AChE: acetylcholinesterase; Apt: aptamer; CTAB: cetyltrimethylammonium bromide; QD: quantum dots.

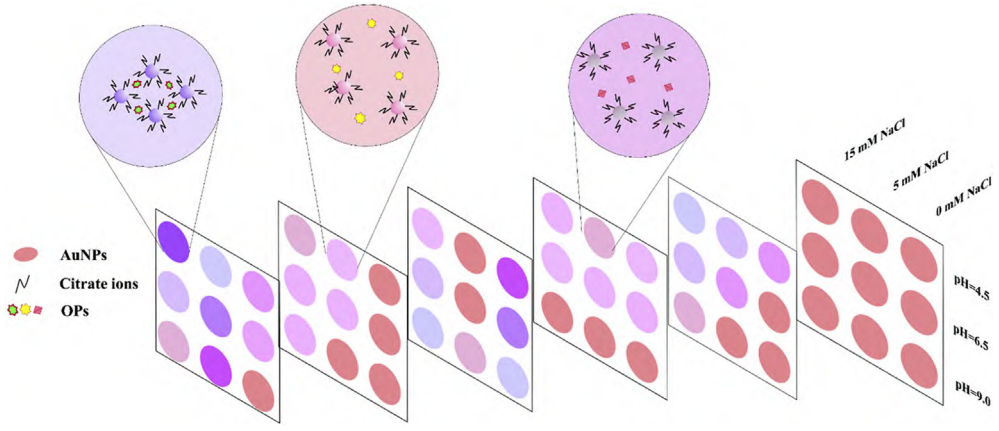

Fig. 4. Diagrams of colorimetric sensor array and detection principle of Organophosphorus pesticides based on unmodified AuNPs. Reproduced with permission from Ref. [103].

naked eyes with a limit of detection of 35 ppb. A combined analytical method by utilizing dispersive liquid-liquid microextraction and AuNPs as a colorimetric sensor based on in situ formation of AuNPs in carbon tetrachloride as an organic phase was developed for the detection of zineb [109] and ziram [110]. Modified small molecules on the surface of AuNPs can improve their selectivity and sensitivity. Thus, Kang et al. [111] have demonstrated pymetrozine-induced aggregation of melamine-AuNPs as a colorimetric sensor. The addition of pymetrozine caused the aggregation of melamine-AuNPs, indicating a color change from red to blue. Wang et al. [112] modified AuNPs with 2-mercapto-6-nitrobenzothiazole as colorimetric probes for the detection of deltamethrin. Tu et al. [113] employed cysteamine-modified AuNPs to probe glyphosate in aqueous solution. The presence of glyphosate induced the aggregation of AuNPs accompanied with the color change from red to blue. The glyphosate spiked spinach, apple, and corn leaves were visualized by the naked eye. Kailasa et al. [114] developed 6-aza-2-thiothymine functionalized AuNPs to probe pencycuron. The sensing mechanism involves the hydrogen bonding, π-π, and van der Waal interactions between pencycuron and 6-aza-2-thiothymine functionalized AuNPs, leading to a change in color from red to blue. The designed AuNPs-based colorimetric sensor has been applied for quantitative determination of pencycuron in rice, potato, cabbage, and water samples. According to the above discussions, label-free AuNPs are sensitive to change in ionic strength and pH of the buffer and other inorganic and organic analytes with high affinity to AuNPs. The labeling AuNPs provide more interactions between target analytes and probe labeled AuNPs with high specificity and sensitivity.

3.2. Fluorescence assays

Fluorescence-based sensors are performed mainly based on the quenching (turn-off) and enhancement (turn-on) of fluorescence intensity, or the fluorescence resonance energy transfer (FRET) [115]. AuNPs can act as highly efficient fluorescence quenchers, owing to the high molar extinction coefficients and broad adsorption spectrum overlapping [116]. The interactions between fluorescent molecules and AuNPs cause the change of the fluorescence intensity. Thus, AuNPs can be utilized as excellent fluorescence quenchers for FRET- and IFE-based assays for the determination of pesticides, as shown in Table 2. Nebu et al. [117] demonstrated that fluorescein-capped AuNPs were sensitive for fluorescence turn-on detection of fenitrothion. As shown in Fig. 5, the fluorescence of fluorescein was quenched by AuNPs and recovered in the presence of fenitrothion. The approach was successfully demonstrated on a paper strip with the detection limit in the nanomolar range. Hung et al. [118] developed a rhodamine B (RB)-functionalized AuNPs as fluorescence "turn-on" probe for the determination of dimethoate. The sensing mechanism is based on the emission spectrum of RB significantly overlaps with the absorption spectrum of AuNPs. In the presence of dimethoate, the fluorescence was recovered owing to the competitive adsorption between RB molecules and dimethoate on the surface of AuNPs. The approach has been applied to detect dimethoate in water and fruit samples with satisfactory recoveries. Tseng et al. [119] used a similar strategy to detect thiodicarb in water and food samples. Su et al. [120] used carbendazim-specific aptamer as a sensing probe, AuNPs, and RB as the indicator to develop an aptasensor for the detection of carbendazim. The aptamer can specifically be combined with carbendazim to form a stable complex and desorbed from the surface of AuNPs, induced the aggregation of AuNPs by NaCl. Bahreyni et al. [121] developed a fluorometric aptasensor to detect acetamiprid based on the use of an aptamer against acetamiprid, different complementary strands, and AuNPs. Except for organic dyes, upconversion nanoparticles, quantum dots, and carbon dots have been proved to be efficient fluorescence donors in recent years. You et al. [122] constructed a competitive immunoassay for the detection of midacloprid by using AuNPs as an absorber for the fluorescence of upconversion nanoparticles through inner filter effect. Yang et al. [123] demonstrated a colorimetric and fluorometric method based on the principle of target-triggered structure switch of aptamers, salt-induced AuNPs aggregation, and signal amplification from upconversion nanoparticles for the detection of acetamiprid. Liu et al. [124] developed a fluorescence turn-on method base on the luminescence resonance energy transfer between upconversion nanoparticles, and AuNPs for the detection of cyano-containing pesticides (acetamiprid, fenpropathrin, and chlorothalonil). The approach also has been applied to detect acetamiprid in *Lanceolata, Angelica dahurica* and *Astragalus*. Dong et al. [102] developed a dual strategy for the fluorescent and visual detection of cyanazine based on the quantum dots (QDs)-AuNPs sensing system. The fluorescence of CdTe QDs was remarkably quenched by AuNPs *via* the inner filter effect (IFE). Upon addition of cyanazine can adsorb on the surface of AuNPs to

Table 2. AuNPs based fluorometric sensors for pesticide detection.

Pesticides	Probes	Linear ranges	LODs	Matrix	Ref.
Fenitrothion	Fluorescein-AuNPs	–	6.05 nM 9.41 nM 7.84 nM	Well water, Tap water, River water	[117]
Dimethoate	RB-AuNPs	0.005–1.0 μg/mL	0.004 μg/mL	Water, Fruit, Rice, Vegetable, Tea	[118]
Thiodicarb	RB-AuNPs	0.1–10.0 μg/mL	0.08 μg/mL	Water, Fruit, Rice	[119]
Carbendazim	RB-Apt-AuNPs	2.33–800 nM	2.33 nM	Water	[120]
Acetamiprid	Apt, Apt-AuNPs	5–50 nM	2.8 nM	Tap water	[121]
Imidaclothiz	UNCPs, AuNPs	2.1–171.2 ng/mL	2.1 ng/mL	Paddy water, Soil, Ear, Rice, Apple, Tomato, Pakchoi, Cabbage	[122]
Acetamiprid	UNCPs, Apt-AuNPs	0.025–1 μM	0.36 nM 0.00008 μg/mL	Celery leaves, Green tea	[123]
Acetamiprid Fenpropathrin Chlorothalonil	UCNPs, Apt-AuNPs	0.10–100 ng/mL 1.0–100 ng/mL 0.10–50 ng/mL	0.015 ng/mL 0.24 ng/mL 0.011 ng/mL	Herbal medicine	[124]
Cyanazine	QDs, AuNPs	0.5–9 μM	0.1578 μM	–	[102]
Acetamiprid	QDs, Apt-AuNPs	0.05–1.0 μM	7.29 nM	Lettuce, Pakchoi, Cauliflower, Pamphrey	[125]
Acetamiprid	CDs, Apt-AuNPs	5–100 ng/mL	1.08 ng/mL	Vegetable	[126]
Acetamiprid	CDs, Apt-AuNPs	7.8 nM–1.4 μM	1.5 nM	Water	[127]
Paraoxon Malathion Methamidophos Carbaryl	CQDs, AuNPs	0.16–5 nM 10–500 nM 10–500 nM 10–666 nM	50 pM 0.1 nM 0.12 nM 0.13 nM	Tap Water, River water, Apple juice	[128]
Paraoxon	PTDNP, AuNPs	0.8–60 ng/mL	0.38 ng/mL	Lake water, Cabbage	[129]

Apt: aptamer; CDs: carbon dots; CQDs: carbon quantum dots; PTDNP: aggregation-induced emission amphiphilic polymers nanoparticles; RB: rhodamine B; QDs: quantum dots; UCNPs: upconversion nanoparticles.

induce the aggregation of AuNP, and the weakened IFE recovered the fluorescence intensity of CdTe QDs. Guo et al. [125] reported a fluorescent assay for acetamiprid based on the specific binding of aptamers and the inner filter effect of AuNPs on the fluorescence of CdTe quantum dots. On the other hand, carbon dots characterize excellent aqueous solubility, resistance to photobleaching, bright fluorescence, low toxicity and good biocompatibility and act as good alternative to organic dyes. Wang et al. [126] reported a fluorescent aptasensor based on the IFE between AuNPs and carbon dots for the detection of acetamiprid. Upon adding acetamiprid, the fluorescence intensity can be recovered and proportioned to the concentration of acetamiprid. Qin et al. [127] developed an aptasensor based on the different aggregation states of AuNPs to quench the fluorescent carbon dots to detect acetamiprid. The assay has been used to detect acetamiprid in rice field water samples. Korram et al. [128]. Constructed a FRET sensing probe using carbon quantum dots and AuNPs for the detection of paraoxon, malathion, methamidophos, and carbaryl. The fluorescence of carbon quantum dots was quenched

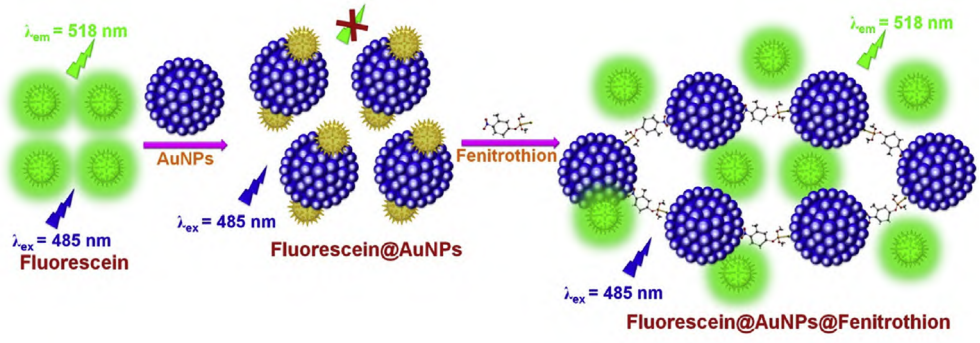

Fig. 5. The schematic representation of the mechanism of quenching of fluorescein by AuNPs and turn-on response of AuNPs quenched fluorescein in the presence of fenitrothion. Reproduced with permission from Ref. [117].

in the presence of AuNPs and recovered by the addition of acetylthiocholine iodide and AChE. By evaluating the inhibition effect on the activity of acetylthiocholine and fluorescence intensity, the concentration of pesticides could be quantified. Chen et al. [129] demonstrated a sensing system consisted of aggregation-induced emission (AIE) NPs, AuNPs, and AChE for the detection of paraoxon. The sensing platform was proved to have a wider linear range from 0.8 to 60 ng/mL with a LOD at 0.38 ng/mL.

3.3. Surface-enhanced Raman scattering assays

Surface-enhanced Raman scattering (SERS) is based on a significant enhancement of Raman signal, typically up to 6 orders of magnitude, from a rough metal surface owing to the electromagnetic and chemical enhancement [130]. Nanostructured surfaces of gold, silver, or copper are the most common SERS-active substrates. SERS provides the characteristic fingerprint of desirable analytes with high sensitivity at nanomolar to picomolar concentration, even at the single-molecule level [131–133]. Thus, SERS has become a powerful analytical method for detecting pesticides because of its high sensitivity, good selectivity, low cost, and rapidity [134,135].

Recently, Xu et al. reviewed the development of the SERS technique for pesticide detection in food with the advantages of high sensitivity, reproducibility, selectivity, and low-cost [136]. The liquid samples can be directly detected for pesticide residues by SERS (Fig. 6a); the pesticide residues on the surface of a solid or solid-liquid mixture can be detected by SERS (Fig. 6b); the pesticide residues inside solid sample also can be detected by SERS with an extraction process (Fig. 6c). Thus, the following are recent achievements in fabricating appropriate SERS-active substrates for pesticide detection. In recent year, several pesticides such as omethoate [137], chlorpyrifos [137], acetamiprid [138], clothianidin [138], phosmet [138], thiram [138], paraquat [139], carbendazim [140], pyrimethanil [141] was determined by SERS with easy-to-prepare AuNPs as shown in Table 3. Fernandes et al. [142] used dendrimer stabilized anisotropic AuNPs as SERS probes for the detection of sodium diethyldithiocarbamate, thiram, and paraquat in water. Tan et al. [143]. Demonstrated that osmium carbonyl-clusters binging on the AuNPs as a SERS probe to enhance CO stretching vibration signal and avoid the interference of biomolecule. The probe has been used for highly sensitive detection of glyphosate in spiked beer. Hong et al. [144] used a

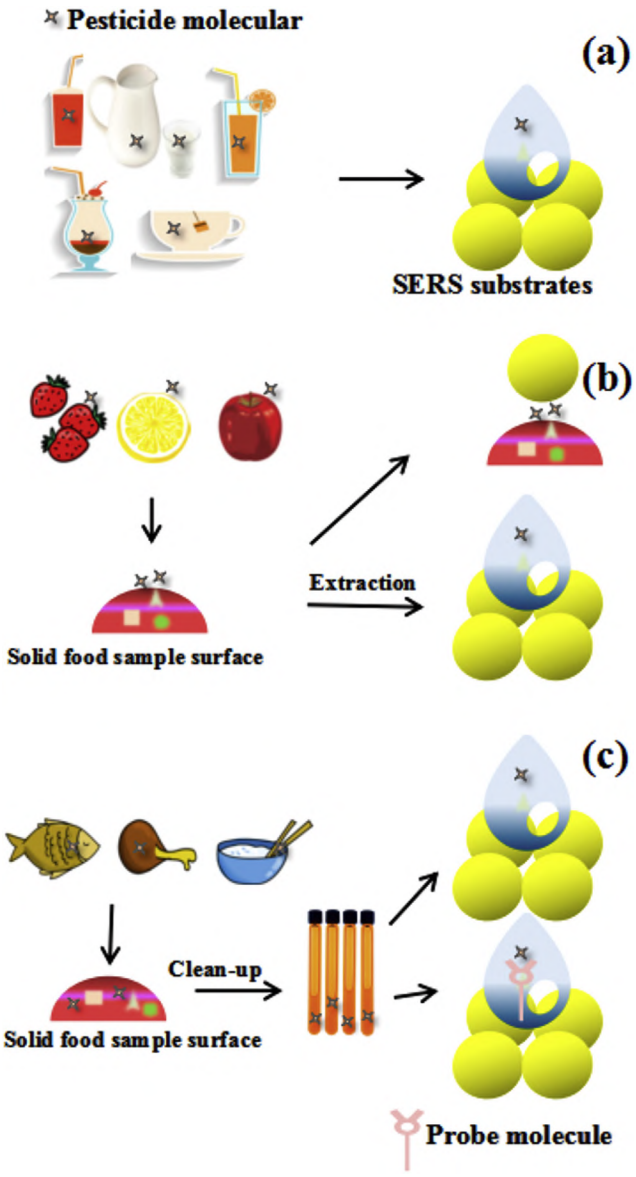

Fig. 6. Pesticide residues detection in liquid (a), on the surface (b), or inside solid foods by SERS. Reproduced with permission from Ref. [136].

suction method to fabricate a SERS substrate *via* the immobilization of AuNPs on an ultrafiltration membrane. The thiabendazole standard solution and orange peel extract can be concentrated on the substrate and analyzed by portable Raman spectrometry. Luo et al. [145] performed AuNPs were in situ synthesized on pseudo-paper films and used as a SERS substrate for the analysis thiram and parathion methyl with 3.02×10^6 enhancement. Yaseen et al. [146] demonstrated a simultaneously detect multi-class pesticides (thiacloprid, profenofos and oxamyl) in peach with SERS on silver-coated AuNPs with 26 nm Au core size and 6 nm Ag shell

Table 3. AuNPs based sensors for pesticide detection by SERS.

Pesticides	Substrates	Linear ranges	LODs	Matrix	Ref.
Omethoate Chlorpyrifos	AuNPs	51.2 – 263 g/L	1.63 mg/cm^2, 2.64 mg/cm^2	Apple	[137]
Acetamiprid, Clothianidin, Imidacloprid, Thiamethoxam, Carbophenothion, Chlorpyrifos, Coumaphos, Malathion, Phosalone, Phosmet, Profenofos, Diphenylamine, Fludioxonil, Thiabendazole, Thiram, Carbofuran, Methomyl, Permethrin, Transfluthrin, Trichlorfon, DEET	AuNPs	–	0.001 – 1 ppm	–	[138]
Paraquat	AuNPs	0.2 – 10 μg/L	–	Apple juice	[139]
Carbendazim	AuNPs	0 – 10 ppm	–	Oolong tea	[140]
pyrimethanil	AuNPs	0 – 40 mg/kg	4.74 ppm	Pome fruit	[141]
Diethyldithiocarbamate Thiram Paraquat	Dendirmer-AuNPs	–	10 nM	–	[142]
Glyphosate	^{10Os}CO-Au NPs	0 – 0.1 ppm	0.1 ppb	Beer	[143]
Thiabendazole	immobilization of AuNPs on UF membrane	0.001 – 100 ppm	0.01 μg/mL (standard) 0.125 ppm (orange extract)	Orange extract	[144]
Thiram Parathion methyl	AuNPs on PPFs	10 – 100000 ng/cm^2	1.1 ng/cm^2	Apple peels	[145]
Thiacloprid, Profenofos, Oxamyl	Au@Ag NPs	–	0.01 mg/L (thiacloprid) 0.001 mg/L (profenofos) 0.001 mg/L (oxamyl)	Peach extract	[146]
2,4-D, Pymetrozine, Thiamethoxam	well-ordered AuNPs@MSF	0.01 – 100 ng/mL 0.1 – 1000 ng/mL 0.1 – 1000 ng/mL	0.79 pg/mL. 1.04 pg/mL 1.21 pg/mL	Tap water, Apple, Milk	[147]
Thiram, Tricyclazole	CNF/AuNP nanocomposites	–	1 pM (0.3 ppt) 10 pM (2.4 ppt)	Apple peel, Plant leaf	[148]

^{10Os}CO: organometallic osmium carbonyl clusters; CNF: cellulose nanofiber; DEET: N,N-diethyl-meta-toluamide; MSF: mesoporous silica film; PPFs: pseudo-paper films; UF: Ultrafiltration.

Table 4. AuNPs based electrochemical sensors for pesticide detection.

Pesticides	Probes	Linear ranges	LODs	Matrix	Ref.
Malathion	AChE/Nafion/AuNPs/rGO/GCE	0.0001−1 ng/mL	0.0278 pg/mL (0.084 pM)	Tap water, Mineral water, Chinese cabbage	[154]
Methyl parathion			0.0217 pg/mL (0.0824 pM)		
Paraoxon-ethyl	AChE/MWCNTs-CS/AuNPs/SPCE	0.01−10 μg/mL	0.03 μg/mL	Spinach	[155]
		10−100 μg/mL			
Malathion	GCE/P-ABSA/DAR/AuNPs/DAR/AChE	0.003−30 pM	0.0016 pM	Tap water, Well water, Chinese cabbage	[156]
Methyl parathion		0.0038−38 pM	0.0022 pM		
Methyl parathion	ITO/$(GPDDA/GPSS)_{10}$	0.95−152 μM (0.25−40 ppm)	0.859 μM (0.226 ppm)	Tap water, Soil, Cabbage	[157]
	ITO/$(GPDDA/GPSS)_1(AuNP/GPSS)_{10}$	1.90−228 μM (0.5−60 ppm)	2.930 μM (0.770 ppm)		
Methyl parathion	AuNPs/NR-BSA-graphene/Nafion/GCE	0.02−0.153 μM	6 nM	Soil, Water, Potato juice	[158]
		0.153−1.36 μM			
Methyl parathion	HAuNPs/rGO/GCE	0.3−10 μM	0.12 μM		[159]
Parathion		0.11−50 μM	23 nM		
Simazine	MIP/ATP@AuNPs/ATP/Au electrode	0.03−140 μM	0.012 μM	Tap water, River water, soil	[160]
Tebuconazole	MIP/Au-PB/SH-G/AuNPs/GCE	50 nM−40 mM	12.5 nM	Cucumber, Green vegetable, Strawberry	[161]
Diazinon	Apt/AuNPs/SPGE	0.0304−304 ng/mL	0.005 ng/mL	Rat plasma	[163]
Carbendazim	MCH/Apt/AuNPs/1-AP-CNHs/GCE	0.001−1.0 ng/mL	0.5 pg/mL	Lettuce, Orange juice	[164]
Malathion	Apt/MCH/CP/AuNPs/PDA/GCE	0.5−650 pg/mL	0.5 pg/mL	Cauliflower, Cabbage	[165]
Chlorpyrifos	FTO-AuNPs-chlAb	1 fM - 1 μM	10 fM	Apple, Pomegranate, Cabbage	[166]
Imidacloprid	AuNPs-SPCE	50−10000 pM	22 pM	Tap water, Watermelon, Tomato	[167]

AP-CNHs: 1-aminopyrene modified carbon nanohorns; AChE: acetylcholinesterase; Apt: aptamer; ATP: o-aminothiophenol; AuNPs/rGO: gold nanoparticles/three-dimensional graphene; BSA: bovine serum albumin; chlAb: anti-chlorpyrifos antibodies; CP: capture probe; CS: chitosan; DAR: diazo-resins; FTO: fluorine doped tin-oxide; GCE: glassy carbon electrode; HAuNPs: hollow gold nanoparticles; ITO: indium tin oxide; MCH: 6-mercapto-1-hexanol; MIP: molecularly imprinted polymer; MWCNT: multiwalled carbon nanotube; NR: neutral red; P-ABSA: p-aminobenzenesulfonic acid; PB: Prussian blue; PDA: polydopamine; SH-G: thiol graphene; SPCE: screen-printed carbon electrode.

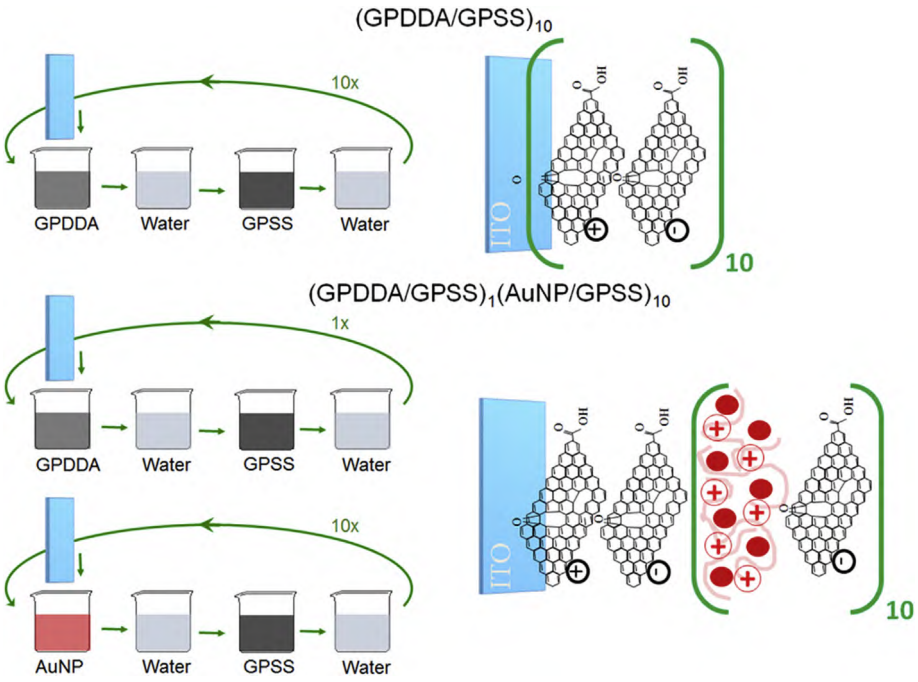

Fig. 7. Procedures to modify ITO electrodes with $(GPPDA/GPSS)_{10}$ and $(GPDDA/GPSS)_1(AuNP/GPSS)_{10}$ LbL films (assembly): immersion time was 15 min for both GPDDA and GPSS, and 6 min for AuNP. Reproduced with permission from Ref. [157].

thickness. Mesoporous silica-supported orderly-spaced AuNPs also used as the SERS substrate for the detection of 2,4-D, pymetrozine and thiamethoxam in food samples [147]. Kim et al. [148] fabricated a low-cost and flexible SERS substrate based on cellulose nanofiber/AuNPs nanocomposites *via* vacuum-assisted filtration. The SERS substrate can effectively detect thiram and tricyclazole with 4.5×10^9 enhancement and LODs were down to 1 pM.

3.4. Electrochemical assays

Electrochemical sensors, because of their portability, rapidity, low-cost, high sensitivity and selectivity, have become one of the most effective analytical methods [149–151]. Electrochemical sensors can be basically divided into potentiometric, amperometric and conductometric methods according to the property of obtained response [152,153]. In recent years, AuNPs have been used for electrochemical sensors for the detection of pesticides as shown in Table 4. Several AuNPs based electrochemical biosensors have been described in the literature by using AChE enzyme [154,155]. Dong et al. [154] developed an AChE sensor for the detection of malathion and parathion methyl in cabbage and water samples based on a film of AuNPs/three-dimensional graphene. Hua et al. [154] demonstrated a disposable amperometric sensor for parathion ethyl determination based on a screen-printed carbon electrode consisted of AChE immobilized onto the surface of multiwalled carbon nanotubes, chitson and AuNPs. Jiang et al. [156] demonstrated to construct stable covalently attached multilayer films by using layer-by-layer self-assembly of diazo-resins, AuNPs, and AChE. The films were immobilized on the surface of a p-aminobenzesulfonic acid-modified glassy carbon electrode and used for quantitative detection of malathion and parathion methyl. Rodrigues et al. [157] performed the fabrication of layer-by-layer films composed of reduced graphene oxide and AuNPs for the detection of parathion methyl (Fig. 7). The differential pulse voltammetry was applied on the layer-by-layer films modified on indium oxide electrode, in the presence of AuNPs, a wider linear range was achieved between 0.5 and 60 ppm, with LOD of 0.770 ppm for parathion methyl. Singh et al. have synthesized the AuNPs/neutral red-BSA-functionalized graphene nanocomposite and immobilized on Nafion modified glassy carbon electrode [158]. The prepared electrode exhibits higher electrocatalytic ability towards methyl parathion with the enlarged current. A sensitive voltammetric sensor for methyl parathion and parathion was developed by Lu et al. [159] based on reduced graphene oxide and hollow AuNPs

immobilized on a glassy carbon electrode. In addition, the molecularly imprinted electrochemical sensors have also used to detect simazine [160] and tebuconazole [161] with AuNPs modified electrodes. Recently, Liu et al. reviewed the development of aptasensor for pesticide detection [162]. Thus, aptasensors based on specific aptamers modified on the AuNPs have been used for the detection of diazinon [163], carbendazim [164] and malathion [165]. Electrochemical immunosensor based on AuNPs have been used for the detection of chlorpyrifos [166] and imidacloprid [167] with ultrahigh sensitivity.

4. Conclusions and future trends

This review has given a brief overview about recent advances of AuNPs-based colorimetric, fluorescence, SERS, and electrochemical sensors for the determination of pesticides in environmental samples. In contrast to conventional chromatographic and mass spectrometry-based methods, AuNPs have been shown to be a very useful, alternative tool for pesticide sensing owing to their unique optical property, facile synthesis, easy surface functionalization, and satisfactory biocompatibility. The selectivity of the AuNP-based probe toward a specific pesticide has been effectively improved by modifying the nanoparticle surface with aptamer and integrating the enzyme-substrate system. However, these reported AuNP-based probes still suffer from some limitations, including the adsorption of non-target molecules on the nanoparticle surface, uncontrolled nanoparticle aggregation in a high-ionic-strength solution, and poor selectivity in complex matrices. Although the modification of AuNPs with neutral surfactants, such as Tween 20 and fluorosurfactant, enhances their colloidal stability in a high-ionic-strength solution, these modifiers provide an adverse effect on selectivity toward a specific pesticide. Additionally, the above-discussed detection methods (i.e., colorimetric, fluorescence, SERS, and electrochemical spectroscopy) are unable to simultaneously sense multiple pesticides with similar structural properties. Therefore, enrichment or separation of the target pesticides would be inevitable prior to using the AuNP-based probe. It is suggested that the integration of the AuNP-based probe with a recognition element-modified platform could be a promising way to allow the detection of target analytes despite of other possible interfering compounds. Examples of recognition elements include aptamer, antibodies, and molecularly imprinted polymers. Also, the integration of the novel technologies such as handheld devices, microfluidic or paper chips and portable test strips with sensing system may promise a bright future for on-site application. The recognition event can be delivered immediately to the servers through wire-less networking and miniaturized device such as smart phone. The applications of AuNPs-based sensors may lead to a new generation in real-time and on-site monitoring pesticides.

Conflict of interest

The authors have declared no conflict of interest.

Acknowledgment

This work was financially supported by the Ministry of Science and Technology of Taiwan, Taiwan under contract number MOST 108-2113-M-017-003 and 109-2113-M-143-002.

References

[1] Thuy PT, Van Geluwe S, Nguyen V-A, Van der Bruggen B. Current pesticide practices and environmental issues in Vietnam: management challenges for sustainable use of pesticides for tropical crops in (South-East) Asia to avoid environmental pollution. J Mater Cycles Waste Manag 2012; 14:379–87.
[2] Marican A, Durán-Lara EF. A review on pesticide removal through different processes. Environ Sci Pollut Res 2018;25: 2051–64.
[3] Gilden RC, Huffling K, Sattler B. Pesticides and health risks. J Obstet Gynecol Neonatal Nurs 2010;39:103–210.
[4] Gorell JM, Johnson C, Rybicki B, Peterson E, Richardson R. The risk of Parkinson's disease with exposure to pesticides, farming, well water, and rural living. Neurology 1998;50: 1346–50.
[5] Tixier P, Chabrier C, Malézieux E. Pesticide residues in heterogeneous plant populations, a model-based approach applied to nematicides in banana (*Musa* spp.). J Agric Food Chem 2007;55:2504–8.
[6] Barra R, Vighi M, Maffioli G, Di Guardo A, Ferrario P. Coupling SoilFug model and GIS for predicting pesticide pollution of surface water at watershed level. Environ Sci Technol 2000;34:4425–33.
[7] Ko E, Choi M, Shin S. Bottom-line mechanism of organochlorine pesticides on mitochondria dysfunction linked with type 2 diabetes. J Hazard Mater 2020;393:122400.
[8] Naous GE-Z, Merhi A, Abboud MI, Mroueh M, Taleb RI. Carcinogenic and neurotoxic risks of acrylamide consumed through caffeinated beverages among the lebanese population. Chemosphere 2018;208:352–7.
[9] Legeay S, Billat P-A, Clere N, Nesslany F, Bristeau S, Faure S, et al. Two dechlorinated chlordecone derivatives formed by in situ chemical reduction are devoid of genotoxicity and mutagenicity and have lower proangiogenic properties compared to the parent compound. Environ Sci Pollut Res 2018;25:14313–23.
[10] Kim K-H, Kabir E, Jahan SA. Exposure to pesticides and the associated human health effects. Sci Total Environ 2017;575: 525–35.
[11] Schurek J, Portolés T, Hajslova J, Riddellova K, Hernández F. Application of head-space solid-phase microextraction coupled to comprehensive two-

dimensional gas chromatography–time-of-flight mass spectrometry for the determination of multiple pesticide residues in tea samples. Anal Chim Acta 2008;611:163–72.
[12] Harshit D, Charmy K, Nrupesh P. Organophosphorus pesticides determination by novel HPLC and spectrophotometric method. Food Chem 2017;230:448–53.
[13] Bala R, Swami A, Tabujew I, Peneva K, Wangoo N, Sharma RK. Ultra-sensitive detection of malathion using quantum dots-polymer based fluorescence aptasensor. Biosens Bioelectron 2018;104:45–9.
[14] Cormode DP, Roessl E, Thran A, Skajaa T, Gordon RE, Schlomka J-P, et al. Atherosclerotic plaque composition: analysis with multicolor CT and targeted gold nanoparticles. Radiology 2010;256:774–82.
[15] El-Sayed IH, Huang X, El-Sayed MA. Surface plasmon resonance scattering and absorption of anti-EGFR antibody conjugated gold nanoparticles in cancer diagnostics: applications in oral cancer. Nano Lett 2005;5:829–34.
[16] Hutter E, Boridy S, Labrecque S, Lalancette-Hébert M, Kriz J, Winnik FM, et al. Microglial response to gold nanoparticles. ACS Nano 2010;4:2595–606.
[17] Schmid G, Corain B. Nanoparticulated gold: syntheses, structures, electronics, and reactivities. Eur J Inorg Chem 2003:3081–98.
[18] Daniel M-C, Astruc D. Gold nanoparticles: assembly, supramolecular chemistry, quantum-size-related properties, and applications toward biology, catalysis, and nanotechnology. Chem Rev 2004;104:293–346.
[19] Mirkin CA, Letsinger RL, Mucic RC, Storhoff JJ. A DNA-based method for rationally assembling nanoparticles into macroscopic materials. Nature 1996;382:607–9.
[20] Elghanian R, Storhoff JJ, Mucic RC, Letsinger RL, Mirkin CA. Selective colorimetric detection of polynucleotides based on the distance-dependent optical properties of gold nanoparticles. Science 1997;277:1078–81.
[21] Huang X, El-Sayed IH, Qian W, El-Sayed MA. Cancer cell imaging and photothermal therapy in the near-infrared region by using gold nanorods. J Am Chem Soc 2006;128:2115–20.
[22] Mastrotto F, Caliceti P, Amendola V, Bersani S, Magnusson JP, Meneghetti M, et al. Polymer control of ligand display on gold nanoparticles for multimodal switchable cell targeting. Chem Commun 2011;47:9846–8.
[23] Walkey CD, Olsen JB, Guo H, Emili A, Chan WC. Nanoparticle size and surface chemistry determine serum protein adsorption and macrophage uptake. J Am Chem Soc 2012;134:2139–47.
[24] Walkey CD, Olsen JB, Song F, Liu R, Guo H, Olsen DWH, et al. Protein corona fingerprinting predicts the cellular interaction of gold and silver nanoparticles. ACS Nano 2014;8:2439–55.
[25] De Jong WH, Hagens WI, Krystek P, Burger MC, Sips AJ, Geertsma RE. Particle size-dependent organ distribution of gold nanoparticles after intravenous administration. Biomaterials 2008;29:1912–9.
[26] Wilhelm S, Tavares AJ, Dai Q, Ohta S, Audet J, Dvorak HF, et al. Analysis of nanoparticle delivery to tumours. Nat Rev Mater 2016;1:1–12.
[27] Turkevich J, Stevenson PC, Hillier J. A study of the nucleation and growth processes in the synthesis of colloidal gold. Discuss Faraday Soc 1951;11:55–75.
[28] Frens G. Controlled nucleation for the regulation of the particle size in monodisperse gold suspensions. Nat Phys Sci (Lond) 1973;241:20–2.
[29] Busbee BD, Obare SO, Murphy CJ. An improved synthesis of high-aspect-ratio gold nanorods. Adv Mater 2003;15:414–6.
[30] Cao C, Park S, Sim SJ. Seedless synthesis of octahedral gold nanoparticles in condensed surfactant phase. J Colloid Interface Sci 2008;322:152–7.
[31] Brust M, Walker M, Bethell D, Schiffrin DJ, Whyman R. Synthesis of thiol-derivatised gold nanoparticles in a two-phase liquid–liquid system. J Chem Soc Chem Commun 1994;801–2.
[32] Sun X, Dong S, Wang E. Large-scale, solution-phase production of microsized, single-crystalline, hexagonal gold microplates by thermal reduction of $HAuCl_4$ with oxalic acid. Chem Lett 2005;34:968–9.
[33] Kumar DR, Kumavat S, Chamundeswari V, Patra PP, Kulkarni A, Prasad B. Surfactant-free synthesis of anisotropic gold nanostructures: can dicarboxylic acids alone act as shape directing agents? RSC Adv 2013;3:21641–7.
[34] Olenic L, Mihailescu G, Pruneanu S, Bratu I, Biris AR, Lupu D, et al. Nanoparticles from a gold complex with sulfite ion as ligand: preparation and characterization. Part Sci Technol 2005;23:79–83.
[35] Yu H, Feng X, Chen X-x, Wang S-s, Jin J. A highly sensitive determination of sulfite using a glassy carbon electrode modified with gold nanoparticles-reduced graphene oxide nano-composites. J Electroanal Chem 2017;801:488–95.
[36] Marişca OT, Leopold N. Anisotropic gold nanoparticle-cell interactions mediated by collagen. Materials 2019;12:1131.
[37] Lévy R, Thanh NT, Doty RC, Hussain I, Nichols RJ, Schiffrin DJ, et al. Rational and combinatorial design of peptide capping ligands for gold nanoparticles. J Am Chem Soc 2004;126:10076–84.
[38] Rahme K, Chen L, Hobbs RG, Morris MA, O'Driscoll C, Holmes JD. PEGylated gold nanoparticles: polymer quantification as a function of PEG lengths and nanoparticle dimensions. RSC Adv 2013;3:6085–94.
[39] Li X, Qin Y, Liu C, Jiang S, Xiong L, Sun Q. Size-controlled starch nanoparticles prepared by self-assembly with different green surfactant: the effect of electrostatic repulsion or steric hindrance. Food Chem 2016;199:356–63.
[40] Chen Y, Xianyu Y, Jiang X. Surface modification of gold nanoparticles with small molecules for biochemical analysis. Acc Chem Res 2017;50:310–9.
[41] Alkilany AM, Abulateefeh SR, Mills KK, Bani Yaseen AI, Hamaly MA, Alkhatib HS, et al. Colloidal stability of citrate and mercaptoacetic acid capped gold nanoparticles upon lyophilization: effect of capping ligand attachment and type of cryoprotectants. Langmuir 2014;30:13799–808.
[42] Godoy-Reyes TM, Costero AM, Gaviña P, Martínez-Máñez R, Sancenón F. Colorimetric detection of normetanephrine, a pheochromocytoma biomarker, using bifunctionalised gold nanoparticles. Anal Chim Acta 2019;1056:146–52.
[43] Liu C-Y, Tseng W-L. Using polysorbate 40-stabilized gold nanoparticles in colorimetric assays of hydrogen cyanide in cyanogenic glycoside-containing plants. Anal Methods 2012;4:2537–42.
[44] Yoon Y-J, Kang S-H, Do C, Moon SY, Kim T-H. Water-redispersible and highly stable gold nanoparticles permanently capped by charge-controllable surfactants for potential medical applications. ACS Appl Nano Mater 2019;2:7924–32.
[45] Ribeiro CA, Albuquerque LJ, de Castro CE, Batista BL, de Souza AL, Albuquerque BL, et al. One-pot synthesis of sugar-decorated gold nanoparticles with reduced cytotoxicity and enhanced cellular uptake. Colloids Surf A Physicochem Eng Asp 2019;580:123690.
[46] Green M, Smyth-Boyle D. Directed growth of gold nanostructures using a nucleoside/nucleotide. J Mater Chem 2007;17:3588–90.
[47] Pu F, Ren J, Qu X. Nucleobases, nucleosides, and nucleotides: versatile biomolecules for generating functional nanomaterials. Chem Soc Rev 2018;47:1285–306.
[48] Cano I, Chapman AM, Urakawa A, van Leeuwen PW. Air-stable gold nanoparticles ligated by secondary phosphine oxides for the chemoselective hydrogenation of aldehydes: crucial role of the ligand. J Am Chem Soc 2014;136:2520–8.
[49] Huang X, Wu H, Liao X, Shi B. One-step, size-controlled synthesis of gold nanoparticles at room temperature using plant tannin. Green Chem 2010;12:395–9.

[50] Sardar R, Shumaker-Parry JS. Spectroscopic and microscopic investigation of gold nanoparticle formation: ligand and temperature effects on rate and particle size. J Am Chem Soc 2011;133:8179–90.
[51] Kundu S, Wang K, Liang H. Size-selective synthesis and catalytic application of polyelectrolyte encapsulated gold nanoparticles using microwave irradiation. J Phys Chem C 2009;113:5157–63.
[52] Agasti SS, Chompoosor A, You C-C, Ghosh P, Kim CK, Rotello VM. Photoregulated release of caged anticancer drugs from gold nanoparticles. J Am Chem Soc 2009;131: 5728–9.
[53] Jana NR, Gearheart L, Murphy CJ. Seeding growth for size control of 5–40 nm diameter gold nanoparticles. Langmuir 2001;17:6782–6.
[54] Murphy CJ, Sau TK, Gole AM, Orendorff CJ, Gao J, Gou L, et al. Anisotropic metal nanoparticles: synthesis, assembly, and optical applications. J Phys Chem B 2005;109:13857–70.
[55] Abécassis B, Testard F, Spalla O, Barboux P. Probing in situ the nucleation and growth of gold nanoparticles by small-angle X-ray scattering. Nano Lett 2007;7:1723–7.
[56] Nehl CL, Liao H, Hafner JH. Optical properties of star-shaped gold nanoparticles. Nano Lett 2006;6:683–8.
[57] Amendola V, Pilot R, Frasconi M, Maragò OM, Iatì MA. Surface plasmon resonance in gold nanoparticles: a review. J Phys Condens Matter 2017;29:203002.
[58] Liu J, Murphy KE, MacCuspie RI, Winchester MR. Capabilities of single particle inductively coupled plasma mass spectrometry for the size measurement of nanoparticles: a case study on gold nanoparticles. Anal Chem 2014;86: 3405–14.
[59] Xu X, Chen J, Li B, Tang L, Jiang J. Single particle ICP-MS-based absolute and relative quantification of *E. coli* O157 16S rRNA using sandwich hybridization capture. Analyst 2019;144:1725–30.
[60] Stolarczyk EU, Stolarczyk K, Łaszcz M, Kubiszewski M, Maruszak W, Olejarz W, et al. Synthesis and characterization of genistein conjugated with gold nanoparticles and the study of their cytotoxic properties. Eur J Pharm Sci 2017;96: 176–85.
[61] Sweeney SF, Woehrle GH, Hutchison JE. Rapid purification and size separation of gold nanoparticles *via* diafiltration. J Am Chem Soc 2006;128:3190–7.
[62] Verma HN, Singh P, Chavan R. Gold nanoparticle: synthesis and characterization. Vet World 2014;7:72–7.
[63] De Souza CD, Nogueira BR, Rostelato MEC. Review of the methodologies used in the synthesis gold nanoparticles by chemical reduction. J Alloys Compd 2019; 798:714–40.
[64] Jana NR, Gearheart L, Murphy CJ. Evidence for seed-mediated nucleation in the chemical reduction of gold salts to gold nanoparticles. Chem Mater 2001;13:2313–22.
[65] Yu Y-Y, Chang S-S, Lee C-L, Wang CC. Gold nanorods: electrochemical synthesis and optical properties. J Phys Chem B 1997;101:6661–4.
[66] Mohamed MB, Ismail KZ, Link S, El-Sayed MA. Thermal reshaping of gold nanorods in micelles. J Phys Chem B 1998;102:9370–4.
[67] Ma H, Yin B, Wang S, Jiao Y, Pan W, Huang S, et al. Synthesis of silver and gold nanoparticles by a novel electrochemical method. ChemPhysChem 2004;5:68–75.
[68] Wei Z, Liu C-j. Synthesis of monodisperse gold nanoparticles in ionic liquid by applying room temperature plasma. Mater Lett 2011;65:353–5.
[69] Wei G-T, Yang Z, Lee C-Y, Yang H-Y, Wang CC. Aqueous–organic phase transfer of gold nanoparticles and gold nanorods using an ionic liquid. J Am Chem Soc 2004;126: 5036–7.
[70] Singh P, Kumari K, Katyal A, Kalra R, Chandra R. Synthesis and characterization of silver and gold nanoparticles in ionic liquid. Spectrochim Acta Mol Biomol Spectrosc 2009; 73:218–20.
[71] Song JY, Jang H-K, Kim BS. Biological synthesis of gold nanoparticles using Magnolia kobus and Diopyros kaki leaf extracts. Process Biochem 2009;44:1133–8.
[72] Gardea-Torresdey J, Parsons J, Gomez E, Peralta-Videa J, Troiani H, Santiago P, et al. Formation and growth of Au nanoparticles inside live alfalfa plants. Nano Lett 2002;2: 397–401.
[73] Iravani S. Green synthesis of metal nanoparticles using plants. Green Chem 2011;13:2638–50.
[74] Polte JR, Ahner TT, Delissen F, Sokolov S, Emmerling F, Thünemann AF, et al. Mechanism of gold nanoparticle formation in the classical citrate synthesis method derived from coupled in situ XANES and SAXS evaluation. J Am Chem Soc 2010;132:1296–301.
[75] El-Sayed IH, Huang X, El-Sayed MA. Selective laser photothermal therapy of epithelial carcinoma using anti-EGFR antibody conjugated gold nanoparticles. Cancer Lett 2006; 239:129–35.
[76] Kumar S, Gandhi K, Kumar R. Modeling of formation of gold nanoparticles by citrate method. Ind Eng Chem Res 2007;46:3128–36.
[77] Patungwasa W, Hodak JH. pH tunable morphology of the gold nanoparticles produced by citrate reduction. Mater Chem Phys 2008;108:45–54.
[78] Li C, Li D, Wan G, Xu J, Hou W. Facile synthesis of concentrated gold nanoparticles with low size-distribution in water: temperature and pH controls. Nanoscale Res Lett 2011;6:440.
[79] Bai W, Zhu C, Liu J, Yan M, Yang S, Chen A. Gold nanoparticle–based colorimetric aptasensor for rapid detection of six organophosphorous pesticides. Environ Toxicol Chem 2015;34:2244–9.
[80] Wang P, Wan Y, Ali A, Deng S, Su Y, Fan C, et al. Aptamer-wrapped gold nanoparticles for the colorimetric detection of omethoate. Sci China Chem 2016;59:237–42.
[81] Lin J-H, Huang K-H, Zhan S-W, Yu C-J, Tseng W-L, Hsieh M-M. Inhibition of catalytic activity of fibrinogen-stabilized gold nanoparticles *via* thrombin-induced inclusion of nanoparticle into fibrin: application for thrombin sensing with more than 10^4-fold selectivity. Spectrochim Acta Mol Biomol Spectrosc 2019;210:59–65.
[82] Yeh P-R, Tseng W-L. Human serum albumin-coated gold nanoparticles for selective extraction of lysozyme from real-world samples prior to capillary electrophoresis. J Chromatogr A 2012;1268:166–72.
[83] Hung S-Y, Shih Y-C, Tseng W-L. Tween 20-stabilized gold nanoparticles combined with adenosine triphosphate-BODIPY conjugates for the fluorescence detection of adenosine with more than 1000-fold selectivity. Anal Chim Acta 2015;857:64–70.
[84] Shih Y-C, Ke C-Y, Yu C-J, Lu C-Y, Tseng W-L. Combined Tween 20-stabilized gold nanoparticles and reduced graphite oxide–Fe_3O_4 nanoparticle composites for rapid and efficient removal of mercury species from a complex matrix. ACS Appl Mater Interfaces 2014;6:17437–45.
[85] Li X, Cui H, Zeng Z. A simple colorimetric and fluorescent sensor to detect organophosphate pesticides based on adenosine triphosphate-modified gold nanoparticles. Sensors 2018;18:4302.
[86] Satnami ML, Korram J, Nagwanshi R, Vaishanav SK, Karbhal I, Dewangan HK, et al. Gold nanoprobe for inhibition and reactivation of acetylcholinesterase: an application to detection of organophosphorus pesticides. Sens Actuator B-Chem 2018;267:155–64.
[87] Sun J, Guo L, Bao Y, Xie J. A simple, label-free AuNPs-based colorimetric ultrasensitive detection of nerve agents and highly toxic organophosphate pesticide. Biosens Bioelectron 2011;28:152–7.
[88] Rohit JV, Basu H, Singhal RK, Kailasa SK. Development of p-nitroaniline dithiocarbamate capped gold nanoparticles-based microvolume UV–vis spectrometric method for facile and selective detection of quinalphos insecticide in

environmental samples. Sens Actuator B-Chem 2016;237: 826–35.
[89] D'souza SL, Pati RK, Kailasa SK. Ascorbic acid functionalized gold nanoparticles as a probe for colorimetric and visual read-out determination of dichlorvos in environmental samples. Anal Methods 2014;6:9007–14.
[90] Park Y, Im A, Hong YN, Kim C-K, Kim YS. Detection of malathion, fenthion and methidathion by using heparin-reduced gold nanoparticles. J Nanosci Nanotechnol 2011;11: 7570–8.
[91] Barman G, Maiti S, Laha JK. Trichloroacetic acid assisted synthesis of gold nanoparticles and its application in detection and estimation of pesticide. J Anal Sci Technol 2013;4:1–7.
[92] Ellman GL, Courtney KD, Andres Jr V, Featherstone RM. A new and rapid colorimetric determination of acetylcholinesterase activity. Biochem Pharmacol 1961;7:88–95.
[93] Chen H, Zhou K, Zhao G. Gold nanoparticles: from synthesis, properties to their potential application as colorimetric sensors in food safety screening. Trends Food Sci Technol 2018;78:83–94.
[94] Xu Q, Du S, Li H, Hu XY. Determination of acetamiprid by a colorimetric method based on the aggregation of gold nanoparticles. Microchim Acta 2011;173:323–9.
[95] Ellington AD, Szostak JW. In vitro selection of RNA molecules that bind specific ligands. Nature 1990;346: 818–22.
[96] Ellington AD, Szostak JW. Selection in vitro of single-stranded DNA molecules that fold into specific ligand-binding structures. Nature 1992;355:850–2.
[97] Tuerk C, Gold L. Systematic evolution of ligands by exponential enrichment: RNA ligands to bacteriophage T4 DNA polymerase. Science 1990;249:505–10.
[98] Weerathunge P, Ramanathan R, Shukla R, Sharma TK, Bansal V. Aptamer-controlled reversible inhibition of gold nanozyme activity for pesticide sensing. Anal Chem 2014; 86:11937–41.
[99] Bala R, Sharma RK, Wangoo N. Development of gold nanoparticles-based aptasensor for the colorimetric detection of organophosphorus pesticide phorate. Anal Bioanal Chem 2016;408:333–8.
[100] Bala R, Dhingra S, Kumar M, Bansal K, Mittal S, Sharma RK, et al. Detection of organophosphorus pesticide–Malathion in environmental samples using peptide and aptamer based nanoprobes. Chem Eng J 2017;311: 111–6.
[101] Yang W, Wu Y, Tao H, Zhao J, Chen H, Qiu S. Ultrasensitive and selective colorimetric detection of acetamiprid pesticide based on the enhanced peroxidase-like activity of gold nanoparticles. Anal Methods 2017;9:5484–93.
[102] Dong L, Hou C, Yang M, Fa H, Wu H, Shen C, et al. Highly sensitive colorimetric and fluorescent sensor for cyanazine based on the inner filter effect of gold nanoparticles. J Nanopart Res 2016;18:164.
[103] Fahimi-Kashani N, Hormozi-Nezhad MR. Gold-nanoparticle-based colorimetric sensor array for discrimination of organophosphate pesticides. Anal Chem 2016;88: 8099–106.
[104] Rana K, Bhamore JR, Rohit JV, Park T-J, Kailasa SK. Ligand exchange reactions on citrate-gold nanoparticles for a parallel colorimetric assay of six pesticides. New J Chem 2018; 42:9080–90.
[105] Baek SH, Lee SW, Kim EJ, Shin D-H, Lee S-W, Park TJ. Portable agrichemical detection system for enhancing the safety of agricultural products using aggregation of gold nanoparticles. ACS Omega 2017;2:988–93.
[106] Ma Y, Jiang H, Shen C, Hou C, Huo D, Wu H, et al. Detection of carbendazim residues with a colorimetric sensor based on gold nanoparticles. J Appl Spectrosc 2017; 84:460–5.
[107] Liu Q, Han P, Gong W, Wang H, Feng X. Colorimetric determination of the pesticide chlorothalonil based on the aggregation of gold nanoparticles. Microchim Acta 2018; 185:354.
[108] Wu S, Li D, Wang J, Zhao Y, Dong S, Wang X. Gold nanoparticles dissolution based colorimetric method for highly sensitive detection of organophosphate pesticides. Sens Actuator B-Chem 2017;238:427–33.
[109] Mohamadjafari S, Rastegarzadeh S. A sensing colorimetric method based on in situ formation of gold nanoparticles after dispersive liquid-liquid microextraction for determination of zineb. Microchem J 2017;132:154–60.
[110] Hashemi F, Rastegarzadeh S, Pourreza N. A combination of dispersive liquid–liquid microextraction and surface plasmon resonance sensing of gold nanoparticles for the determination of ziram pesticide. J Separ Sci 2018;41: 1156–63.
[111] Kang J-y, Zhang Y-j, Li X, Dong C, Liu H-y, Miao L-j, et al. Rapid and sensitive colorimetric sensing of the insecticide pymetrozine using melamine-modified gold nanoparticles. Anal Methods 2018;10:417–21.
[112] Wang Z, Huang Y, Wang D, Sun L, Dong C, Fang L, et al. A rapid colorimetric method for the detection of deltamethrin based on gold nanoparticles modified with 2-mercapto-6-nitrobenzothiazole. Anal Methods 2018;10: 1774–80.
[113] Tu Q, Yang T, Qu Y, Gao S, Zhang Z, Zhang Q, et al. In situ colorimetric detection of glyphosate on plant tissues using cysteamine-modified gold nanoparticles. Analyst 2019;144: 2017–25.
[114] Kailasa SK, Nguyen TP, Baek SH, Rafique R, Park TJ. Assembly of 6-aza-2-thiothymine on gold nanoparticles for selective and sensitive colorimetric detection of pencycuron in water and food samples. Talanta 2019;205:120087.
[115] Jin Y, Gao X. Plasmonic fluorescent quantum dots. Nat Nanotechnol 2009;4:571–6.
[116] Huang C-C, Chang H-T. Selective gold-nanoparticle-based "turn-on" fluorescent sensors for detection of mercury(II) in aqueous solution. Anal Chem 2006;78:8332–8.
[117] Nebu J, Devi JA, Aparna R, Aswathy B, Lekha G, Sony G. Fluorescence turn-on detection of fenitrothion using gold nanoparticle quenched fluorescein and its separation using superparamagnetic iron oxide nanoparticle. Sens Actuator B-Chem 2018;277:271–80.
[118] Hung S-H, Lee J-Y, Hu C-C, Chiu T-C. Gold-nanoparticle-based fluorescent "turn-on" sensor for selective and sensitive detection of dimethoate. Food Chem 2018;260:61–5.
[119] Tseng M-H, Hu C-C, Chiu T-C. A fluorescence turn-on probe for sensing thiodicarb using Rhodamine B functionalized gold nanoparticles. Dyes Pigments 2019;171:107674.
[120] Su L, Wang S, Wang L, Yan Z, Yi H, Zhang D, et al. Fluorescent aptasensor for carbendazim detection in aqueous samples based on gold nanoparticles quenching Rhodamine B. Spectrochim Acta A Mol Biomol Spectros 2020;225: 117511.
[121] Bahreyni A, Yazdian-Robati R, Ramezani M, Abnous K, Taghdisi SM. Fluorometric aptasensing of the neonicotinoid insecticide acetamiprid by using multiple complementary strands and gold nanoparticles. Microchim Acta 2018;185:272.
[122] You H, Hua X, Feng L, Sun N, Rui Q, Wang L, et al. Competitive immunoassay for imidaclothiz using upconversion nanoparticles and gold nanoparticles as labels. Microchim Acta 2017;184:1085–92.
[123] Yang L, Sun H, Wang X, Yao W, Zhang W, Jiang L. An aptamer based aggregation assay for the neonicotinoid insecticide acetamiprid using fluorescent upconversion nanoparticles and DNA functionalized gold nanoparticles. Microchim Acta 2019;186:308.
[124] Liu M, Zhang L, Jiang S, Fu Z. A facile luminescence resonance energy transfer method for detecting cyano-containing pesticides in herbal medicines. Microchem J 2020;152:104451.
[125] Guo J, Li Y, Wang L, Xu J, Huang Y, Luo Y, et al. Aptamer-based fluorescent screening assay for acetamiprid *via* inner

filter effect of gold nanoparticles on the fluorescence of CdTe quantum dots. Anal Bioanal Chem 2016;408:557–66.
[126] Wang J, Wu Y, Zhou P, Yang W, Tao H, Qiu S, et al. A novel fluorescent aptasensor for ultrasensitive and selective detection of acetamiprid pesticide based on the inner filter effect between gold nanoparticles and carbon dots. Analyst 2018;143:5151–60.
[127] Qin X, Lu Y, Bian M, Xiao Z, Zhang Y, Yuan Y. Influence of gold nanoparticles in different aggregation states on the fluorescence of carbon dots and its application. Anal Chim Acta 2019;1091:119–26.
[128] Korram J, Dewangan L, Nagwanshi R, Karbhal I, Ghosh KK, Satnami ML. A carbon quantum dot–gold nanoparticle system as a probe for the inhibition and reactivation of acetylcholinesterase: detection of pesticides. New J Chem 2019;43:6874–82.
[129] Chen J, Chen X, Huang Q, Li W, Yu Q, Zhu L, et al. Amphiphilic polymer-mediated aggregation-induced emission nanoparticles for highly sensitive organophosphorus pesticide biosensing. ACS Appl Mater Interfaces 2019;11:32689–96.
[130] Cai L, Dong J, Wang Y, Chen X. A review of developments and applications of thin-film microextraction coupled to surface-enhanced Raman scattering. Electrophoresis 2019; 40:2041–9.
[131] Laing S, Gracie K, Faulds K. Multiplex *in vitro* detection using SERS. Chem Soc Rev 2016;45:1901–18.
[132] Jiang X, Jiang Z, Xu T, Su S, Zhong Y, Peng F, et al. Surface-enhanced Raman scattering-based sensing *in vitro*: facile and label-free detection of apoptotic cells at the single-cell level. Anal Chem 2013;85:2809–16.
[133] Dasary SS, Singh AK, Senapati D, Yu H, Ray PC. Gold nanoparticle based label-free SERS probe for ultrasensitive and selective detection of trinitrotoluene. J Am Chem Soc 2009;131:13806–12.
[134] Saute B, Premasiri R, Ziegler L, Narayanan R. Gold nanorods as surface enhanced Raman spectroscopy substrates for sensitive and selective detection of ultra-low levels of dithiocarbamate pesticides. Analyst 2012; 137:5082–7.
[135] Xu Q, Guo X, Xu L, Ying Y, Wu Y, Wen Y, et al. Template-free synthesis of SERS-active gold nanopopcorn for rapid detection of chlorpyrifos residues. Sens Actuator B-Chem 2017;241:1008–13.
[136] Xu M-L, Gao Y, Han XX, Zhao B. Detection of pesticide residues in food using surface-enhanced Raman spectroscopy: a review. J Agric Food Chem 2017;65:6719–26.
[137] Chen J, Dong D, Ye S. Detection of pesticide residue distribution on fruit surfaces using surface-enhanced Raman spectroscopy imaging. RSC Adv 2018;8:4726–30.
[138] Dowgiallo A-M, Guenther DA. Determination of the limit of detection of multiple pesticides utilizing gold nanoparticles and surface-enhanced Raman Spectroscopy. J Agric Food Chem 2019;67:12642–51.
[139] Luo H, Wang X, Huang Y, Lai K, Rasco BA, Fan Y. Rapid and sensitive surface-enhanced Raman spectroscopy (SERS) method combined with gold nanoparticles for determination of paraquat in apple juice. J Sci Food Agric 2018;98:3892–8.
[140] Chen X, Lin M, Sun L, Xu T, Lai K, Huang M, et al. Detection and quantification of carbendazim in Oolong tea by surface-enhanced Raman spectroscopy and gold nanoparticle substrates. Food Chem 2019;293:271–7.
[141] Mandrile L, Giovannozzi A, Durbiano F, Martra G, Rossi A. Rapid and sensitive detection of pyrimethanil residues on pome fruits by surface enhanced Raman scattering. Food Chem 2018;244:16–24.
[142] Fernandes T, Fateixa S, Nogueira H, Daniel-da-Silva A, Trindade T. Dendrimer-based gold nanostructures for SERS detection of pesticides in water. Eur J Inorg Chem 2020:1153–62.
[143] Tan MJ, Hong Z-Y, Chang M-H, Liu C-C, Cheng H-F, Loh XJ, et al. Metal carbonyl-gold nanoparticle conjugates for highly sensitive SERS detection of organophosphorus pesticides. Biosens Bioelectron 2017;96:167–72.
[144] Hong J, Kawashima A, Hamada N. A simple fabrication of plasmonic surface-enhanced Raman scattering (SERS) substrate for pesticide analysis *via* the immobilization of gold nanoparticles on UF membrane. Appl Surf Sci 2017; 407:440–6.
[145] Luo W, Chen M, Hao N, Huang X, Zhao X, Zhu Y, et al. In situ synthesis of gold nanoparticles on pseudo-paper films as flexible SERS substrate for sensitive detection of surface organic residues. Talanta 2019;197:225–33.
[146] Yaseen T, Pu H, Sun D-W. Fabrication of silver-coated gold nanoparticles to simultaneously detect multi-class insecticide residues in peach with SERS technique. Talanta 2019; 196:537–45.
[147] Xu Y, Kutsanedzie FY, Hassan M, Zhu J, Ahmad W, Li H, et al. Mesoporous silica supported orderly-spaced gold nanoparticles SERS-based sensor for pesticides detection in food. Food Chem 2020;315:126300.
[148] Kim D, Ko Y, Kwon G, Choo Y-M, You J. Low-cost, high-performance plasmonic nanocomposites for hazardous chemical detection using surface enhanced Raman scattering. Sens Actuator B-Chem 2018;274:30–6.
[149] Niu X, Yang W, Wang G, Ren J, Guo H, Gao J. A novel electrochemical sensor of bisphenol A based on stacked graphene nanofibers/gold nanoparticles composite modified glassy carbon electrode. Electrochim Acta 2013;98: 167–75.
[150] Xue C, Han Q, Wang Y, Wu J, Wen T, Wang R, et al. Amperometric detection of dopamine in human serumby electrochemical sensor based on gold nanoparticles doped molecularly imprinted polymers. Biosens Bioelectron 2013; 49:199–203.
[151] Rezaei B, Boroujeni MK, Ensafi AA. Fabrication of DNA, o-phenylenediamine, and gold nanoparticle bioimprinted polymer electrochemical sensor for the determination of dopamine. Biosens Bioelectron 2015;66:490–6.
[152] Stradiotto NR, Yamanaka H, Zanoni MVB. Electrochemical sensors: a powerful tool in analytical chemistry. J Braz Chem Soc 2003;14:159–73.
[153] Pejcic B, De Marco R. Impedance spectroscopy: over 35 years of electrochemical sensor optimization. Electrochim Acta 2006;51:6217–29.
[154] Dong P, Jiang B, Zheng J. A novel acetylcholinesterase biosensor based on gold nanoparticles obtained by electroless plating on three-dimensional graphene for detecting organophosphorus pesticides in water and vegetable samples. Anal Methods 2019;11:2428–34.
[155] Hua QT, Ruecha N, Hiruta Y, Citterio D. Disposable electrochemical biosensor based on surface-modified screen-printed electrodes for organophosphorus pesticide analysis. Anal Methods 2019;11:3439–45.
[156] Jiang B, Dong P, Zheng J. A novel amperometric biosensor based on covalently attached multilayer assemblies of gold nanoparticles, diazo-resins and acetylcholinesterase for the detection of organophosphorus pesticides. Talanta 2018;183: 114–21.
[157] Rodrigues GH, Miyazaki CM, Rubira RJ, Constantino CJ, Ferreira M. Layer-by-Layer films of graphene nanoplatelets and gold nanoparticles for Methyl Parathion Sensing. ACS Appl Nano Mater 2019;2:1082–91.
[158] Singh M, Kashyap H, Singh PK, Mahata S, Rai VK, Rai A. AuNPs/Neutral red-biofunctionalized graphene nanocomposite for nonenzymatic electrochemical detection of organophosphate *via* NO_2 reduction. Sens Actuator B-Chem 2019;290:195–202.
[159] Lu J, Sun Y, Waterhouse GI, Xu Z. A voltammetric sensor based on the use of reduced graphene oxide and hollow gold nanoparticles for the quantification of methyl parathion and parathion in agricultural products. Adv Polym Technol 2018;37:3629–38.
[160] Zhang J, Wang C, Niu Y, Li S, Luo R. Electrochemical sensor based on molecularly imprinted composite

membrane of poly (o-aminothiophenol) with gold nanoparticles for sensitive determination of herbicide simazine in environmental samples. Sens Actuator B-Chem 2017;249:747–55.

[161] Qi P, Wang J, Wang Z, Wang X, Wang X, Xu X, et al. Construction of a probe-immobilized molecularly imprinted electrochemical sensor with dual signal amplification of thiol graphene and gold nanoparticles for selective detection of tebuconazole in vegetable and fruit samples. Electrochim Acta 2018;274:406–14.

[162] Liu M, Khan A, Wang Z, Liu Y, Yang G, Deng Y, et al. Aptasensors for pesticide detection. Biosens Bioelectron 2019;130:174–84.

[163] Hassani S, Akmal MR, Salek-Maghsoudi A, Rahmani S, Ganjali MR, Norouzi P, et al. Novel label-free electrochemical aptasensor for determination of Diazinon using gold nanoparticles-modified screen-printed gold electrode. Biosens Bioelectron 2018;120:122–8.

[164] Zhu C, Liu D, Chen Z, Li L, You T. An ultra-sensitive aptasensor based on carbon nanohorns/gold nanoparticles composites for impedimetric detection of carbendazim at picogram levels. J Colloid Interface Sci 2019;546:92–100.

[165] Xu G, Hou J, Zhao Y, Bao J, Yang M, Fa H, et al. Dual-signal aptamer sensor based on polydopamine-gold nanoparticles and exonuclease I for ultrasensitive malathion detection. Sens Actuator B-Chem 2019;287:428–36.

[166] Talan A, Mishra A, Eremin SA, Narang J, Kumar A, Gandhi S. Ultrasensitive electrochemical immuno-sensing platform based on gold nanoparticles triggering chlorpyrifos detection in fruits and vegetables. Biosens Bioelectron 2018;105:14–21.

[167] Pérez-Fernández B, Mercader JV, Abad-Fuentes A, Checa-Orrego BI, Costa-García A, de la Escosura-Muñiz A. Direct competitive immunosensor for Imidacloprid pesticide detection on gold nanoparticle-modified electrodes. Talanta 2020;209:120465.